Phased Simulation of a Tunnel Boring process in Soft Soil

Broere, Wout; Brinkgreve, Ronald

Publication date
2002

Document Version
Accepted author manuscript

Published in
NUMGE 2002 : 5th European Conference Numerical Methods in Geotechnical Engineering

Citation (APA)
Broere, W., & Brinkgreve, R. (2002). Phased Simulation of a Tunnel Boring process in Soft Soil. In Mestat (Ed.), *NUMGE 2002 : 5th European Conference Numerical Methods in Geotechnical Engineering* (pp. 529–536)

Numerical Methods in Geotechnical Engineering, Mestat (ed.) 2002, Presses de l'ENPC/LCPC, Paris, pp. 529-536

PHASED SIMULATION OF A TUNNEL BORING PROCESS IN SOFT SOIL

MÓDELISATION PAR ÉTAPES DU CREUSEMENT D'UN TUNNEL EN TERRAIN MEUBLE

W. Broere [1,2], R.B.J. Brinkgreve [2,3]
[1] *A. Broere BV, Amsterdam, The Netherlands*
[2] *Geotechnical Laboratory, Delft University of Technology, Delft, The Netherlands*
[3] *Plaxis BV, Delft, The Netherlands*

ABSTRACT - The advancement of a tunnel boring machine in the ground has been modelled using a phased excavation scheme, including the slurry support at the shield face, the conicity of the shield and the grouting at the shield tail. A comparison is made with field measurements obtained at the Second Heinenoord Tunnel. Also calculations are made including a row of houses, founded on piles, to show the deformations caused by tunnel construction.

RÉSUMÉ – L'avancement d'un tunnelier dans un massif a été modélisé en plusieurs étapes qui prennent en compte le soutènement du front par boue pressurisée, la conicité du bouclier et les injections. Les resultants numériques sont compares aux measures effectuées sur le deuxième tunnel de Heinenoord. D'autres calculs avec simulation d'une rangée de maisons sur pieux ont été menés pour évaluer l'effet des tassements associés à la construction du tunnel.

1. Introduction

The ongoing advancement in the shield tunnelling technique has opened the possibility to construct tunnels in urban areas, even in situations where the technique was deemed unsuited a decade ago. The North-South light rail in Amsterdam is an example of a project where a tunnel will be constructed in close proximity of historical buildings under difficult conditions (Teunissen, 1998). The twin tunnels will be constructed near historical masonry buildings, founded on wooden piles, as well as newer buildings, founded on prefabricated concrete piles. Along the main part of the line the tunnels will run next to or beneath the toes of the wooden foundation piles. Both the piles and the masonry construction itself have little margin for deformation before damage to the construction will occur.

For a correct assessment of the influence of the tunnel boring process on the buildings, and of possible damage to the buildings, a detailed prediction of the soil deformations, caused by the tunnel boring machine (TBM), is needed. Especially the gradient of the settlement trough is a main factor in the damage assessment.

It has been recognised for some time that the settlement trough calculated in cross-sections, using a two-dimensional finite element model, is wider and less steep than those observed in field measurements. The same holds for the settlement trough calculated using analytical methods (Strack, 2000; Verruijt, 2000). Also, it is still difficult to correctly model the influence of the tunnel boring machine in such calculations.

Many attempts to model parts of the tunnel construction process using three-dimensional finite elements have focused mainly on the detailed construction of the tunnel lining, e.g. (van der Vliet 1999). The influence of the surrounding soil on the lining is often schematised using linear springs, and the influence of the tunnel boring process on the surrounding soil is disregarded. The recent advancements in three-dimensional finite element programs do allow for a more detailed analysis of soil deformation during tunnel construction, see for example (Vermeer, 2000).

A phased excavation scheme that can be used in Plaxis 3D Tunnel is presented by (Vermeer, 2001; Brinkgreve, 2001) to simulate the deformations caused by tunnelling. In this Paper this method is first used to postdict the deformations measured during construction of the Second Heinenoord Tunnel. Although the slice-wise input procedure used in Plaxis 3D Tunnel suggests using a constant cross-section, the method can be slightly adapted. In this way it is possible to investigate the effects of discontinuities in the soil or local changes in the geometry. The adapted method will be used to study the influence of tunnel boring on a number of buildings founded on piles.

2. The Second Heinenoord Tunnel

The Second Heinenoord Tunnel is the first large diameter bored tunnel in the Netherlands, constructed in soft soil conditions with a high water table. The tunnel consists of two 8.5 m outer diameter tubes, which were bored beneath the River Oude Maas. As the tunnel was a pilot project, it has been extensively monitored during and after construction. Full details of the test programme are given, amongst others, by (Bakker, 1996). On the North bank of the river an instrumented plot was laid out. The deformations of the soil at this location were monitored using settlement plates, extensometers and inclinometers.

A calculation of the deformations around the TBM at the location of the instrumented plot has been made using a three-dimensional finite element model. In this model one symmetric half of the soil layers, the TBM and the final tunnel lining are modelled. The soil has been schematised as 8 horizontal layers, with their location and properties as listed in Table 1. All layers were modelled using the Mohr-Coulomb model. The soil properties were obtained from the preliminary soil investigation (COB 1996), with the exception of the stiffnesses of the layers below the tunnel. For these layers below the tunnel a high small strain unloading stiffness was used.

Table 1. Soil layers and their parameters (Mohr-Coulomb model)

Layer	Top [m+NAP]	Type	γ_{unsat} [kN/m^3]	γ_{sat} [kN/m^3]	v [-]	E_{ref} [kN/m^2]	c [kN/m^2]	φ [°]	Ψ [°]	K_0 [-]
1	2.50	Undr.	16.5	17.2	0.34	3900	3.0	27.0	0.0	0.58
2	1.00	Drain.	16.5	17.2	0.34	3900	3.0	27.0	0.0	0.58
3	-1.50	Drain.	20.5	20.5	0.30	29600	0.0	36.5	6.5	0.47
2	-5.75	Drain.	19.0	19.0	0.31	18500	0.0	33.0	3.0	0.47
5	-10.00	Drain.	19.5	19.5	0.30	19300	0.0	35.0	5.0	0.45
6	-17.25	Drain.	20.5	20.5	0.30	444000	0.0	36.5	6.5	0.50
7	-20.75	Undr.	20.0	20.0	0.32	119000	7.0	31.0	1.0	0.55
8	-25.00	Drain.	21.0	21.0	0.30	593000	0.0	37.5	7.5	0.56

The hydrostatic pore pressure distribution for the model was derived using a hydrostatic head at 1.0 m+NAP (NAP = the Dutch ordinance datum).

The 3D finite element model used consists of 3440 quadratic volume elements, divided into a number of slices with identical initial geometry (see Figure 2). The first 14 slices are 3.0 m thick in the longitudinal tunnel direction. The last 6 slices increase slightly in thickness, up to 4.13 m for the last slice. The TBM was modelled as a three slice long ring of shell elements. The flexural rigidity of the shell EI = 50 10^3 kNm^2/m and the normal stiffness EA = 10 10^6 kN/m. The weight of the shell is taken as w = 38.15 kN/m^2, representing the full weight of the TBM. The axis of the TBM is located at -12.3 m+NAP. The final concrete tunnel lining was modelled as a 0.35 m thick continuous ring, using volume elements with a volumetric weight γ = 24 kN/m^3, Young's modulus E = 24.6 10^6 kN/m^2 and Poisson's constant v = 0.2.

At the face of the TBM a face pressure is applied to support the soil during excavation. This face pressure is 140 kN/m^2 at the top of the TBM and increases linearly to 259 kN/m^2 at the invert.

The TBM itself is slightly conical. The tail radius is 20 mm less than the front radius, which effect has been modelled using a total contraction of 0.48 vol.%, i.e. a contraction of 0.16% for each of the slices that make up the TBM.

The influence of the grout injection at the shield tail has been modelled using a distributed

Figure 1. Various excavation phases modelled in the phased excavation procedure

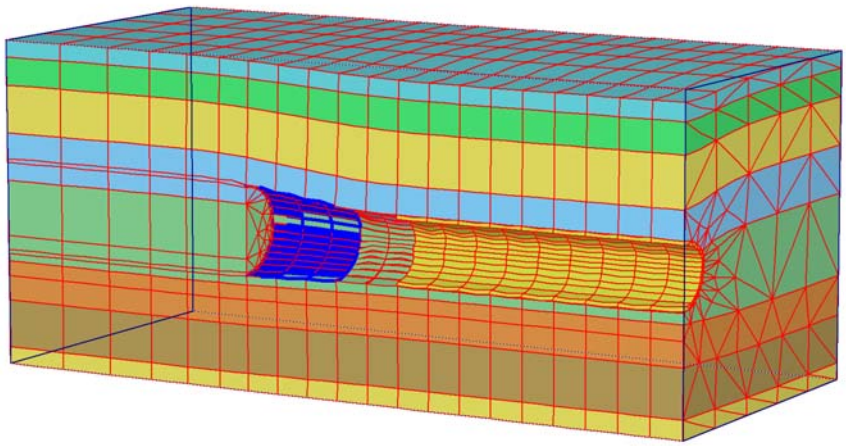

Figure 2. Deformed mesh at the end of Phase 14 (deformations enlarged 50 times)

load, acting over two slices (6 m). Thereafter it is assumed that the grout has settled and dewatered enough that no additional deformations are caused. The grout pressure has been set to 125 kN/m^3 at the top, increasing to 190 kN/m^2 at the bottom. These grouting pressures have been obtained from measurements in the shield annulus. After the grout injection zone the tunnel lining is activated. The various phases of this excavation scheme have been schematised in Figure 1.

The initial stresses are calculated using a coefficient of neutral effective stress K_0 as listed in Table 1 for the various layers. Thereafter the calculation is composed of 14 phases. In the first Phase, the front of the TBM enters the model in the first slice. In each Phase thereafter the TBM progresses into the model. In the fourth phase the grout pressure becomes active for the first time and in the sixth phase the lining is activated. In the final Phase 14 the TBM has progressed 42 m, and no more effects of the starting boundary are observed. The results of the calculations at the end of Phase 14 are presented below.

Figure 2 shows the deformed mesh, with the settlement trough above the tunnel clearly visible. The maximum settlement at the centre line is about 22 mm. In Figures 3 and 4 the results in a cross section 4D (the tunnel diameter) behind the tunnel face are compared to the results

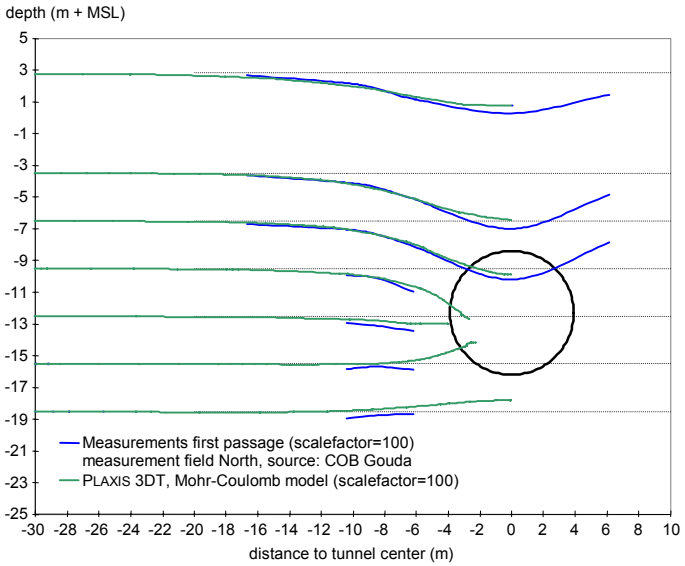

Figure 3. Comparison of the calculated vertical displacements at 4D behind the face with field observations

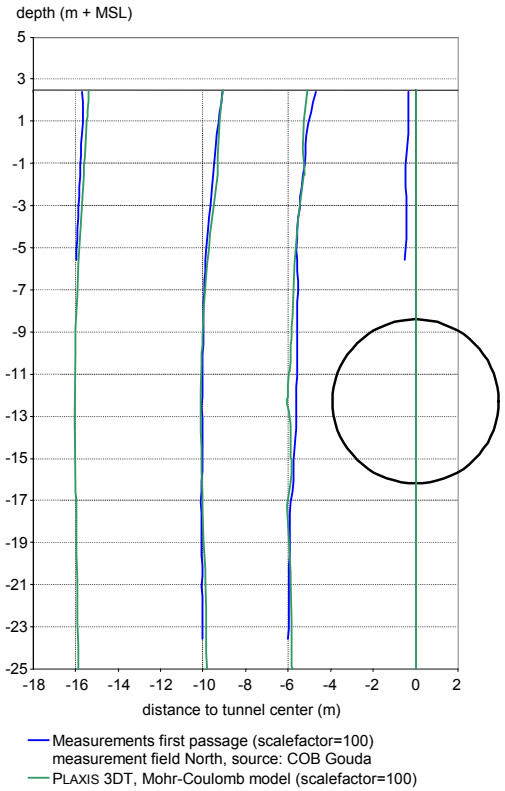

Figure 4. Comparison of the calculated horizontal displacements at 4D behind the face with field observations

obtained from extensometers and inclinometers. The results from the calculations are quite realistic and correspond well to the field measurements.

Not only the width of the settlement trough, but also the deformations at various depths below the surface are calculated quite well. It is interesting to note that the deformations at depth, just above the tunnel crown, are somewhat larger than at the soil surface (up to 38 mm). Also a slight movement towards the tunnel can be observed next to the tunnel. This suggests that the influence of the tunnel boring process on subsurface structures may be larger than predicted using traditional surface settlement predictions. This will be investigated in the next part of this Paper.

Figure 5 shows the shadings of the total displacements at the boundaries of the finite element mesh. This plot confirms the plot of the deformed mesh (Figure 2) and shows in more detail where the largest displacements occur. Also, this plot shows that relatively little displacement occurs below the tunnel, i.e. that the buoyancy of the tunnel is limited.

3. Influence of tunnelling on a building and pile foundation

The influence of tunnelling close to pile foundations on the bearing capacity of those foundations and the resulting deformations of the structures founded on them is still topic of research (Teunissen, 1998). The phased excavation scheme presented above can, with a few adaptations, be used to study this influence. The geometry for this analysis is presented in Figure 6. The most notable difference with the previous case is the inclusion of a row of 3 buildings founded on a total of 12 piles. The houses and piles are modelled using only volume elements. The geometry has been drawn only partially to clearly show the piles foundation.

As Plaxis 3D Tunnel requires the geometry of all slices to be identical, this geometry requires careful meshing in order to limit the total number of elements. Also, in contrast to the Heinenoord case presented above, not all slices have the same thickness. In order to model the

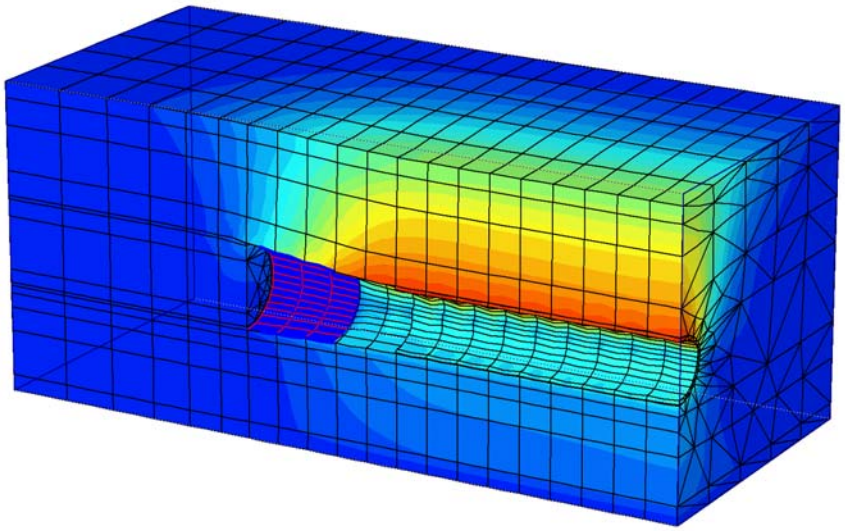

Figure 5. Shadings of total displacements at the end of Phase 14
(deformations enlarged 50 times)

side walls with piles, a number of slices only 0.40 m thick is included, each followed by a 2.60 m thick slice.

The stratification consists of a man-made fill on top of a number of soft layers. The material parameters for the soil layers are given in Table 2. For all layers the Hardening Soil model has been used, with an unloading-reloading stiffness $E_{ur}^{ref} = 3\ E_{50}^{ref}$.

The piles are modelled as 0.40 x 0.40 m linear elastic elements, founded one metre deep in the lower sand layer. The building consists of linear elastic slabs, each 0.40 m thick. Both piles and building have a volumetric weight of 24 kN/m^3. The piles have a Young's modulus $E_{ref} = 3\ 10^6$ kN/m^2 and Poisson's constant v = 0.0. The bulding has been given stiffness parameters representing masonry under shear deformations, $E_{ref} = 1\ 10^6$ kN/m^2 and v = 0.2.

Table 2. Soil and building material parameter sets (Hardening Soil model)

Layer	Top [m]	Type	γ_{unsat} [kN/m^3]	γ_{sat} [kN/m^3]	v [-]	E_{50}^{ref} [kN/m^2]	E_{oed}^{ref} [kN/m^2]	c_{ref} [kN/m^2]	φ [°]	ψ [°]
1	30	Drain.	19.5	19.5	0.2	$30\ 10^3$	$30\ 10^3$	3.0	30.0	0.0
2	27	Drain.	12.0	12.0	0.2	$5\ 10^3$	$5\ 10^3$	7.0	24.0	0.0
3	20	Undr.	16.5	18.5	0.2	$15\ 10^3$	$12\ 10^3$	3.0	27.0	0.0
4	18	Drain.	20.5	20.5	0.2	$40\ 10^3$	$40\ 10^3$	0.0	36.5	6.5

A similar phased excavation scheme as described above has been used. The TBM in this case has a 5 m radius, and the axis at 20 m below the soil surface. The support pressure at the front is 225 kPa at the top of the TBM and increases to 345 kPa at the bottom. The grouting pressure varies between 180 kPa at the top to 260 kPa at the bottom. A 0.40 m thick concrete lining, with E_{ref} = 2.46 107 kN/m2 and v = 0.2 is installed behind the grouting zone.

After the determination of the initial stresses, using the K_0 procedure, first the piles are installed by changing the properties of the clusters from the original soil to those of the piles. Thereafter the building is activated, by switching on the appropriate elements.

As the TBM approaches the row of houses, the corner closest to the TBM naturally starts to settle first. See Figure 7 for a plot of the displacements at this point. The house seems to topple over into the settlement trough, as the front side, closest to the TBM, settles more than the back. The effect is seen strongest as the face of the TBM stands parallel to the last row of piles in Phase 15. At this point the maximum settlement right above the centre line of the tunnel is 24 mm. The closest top corner of the building has moved has moved 23 mm from its original location, made up of 15 mm vertical displacement, 17 mm horizontal displacement towards the symmetry axis of the geometry and 7 mm in the longitudinal direction.

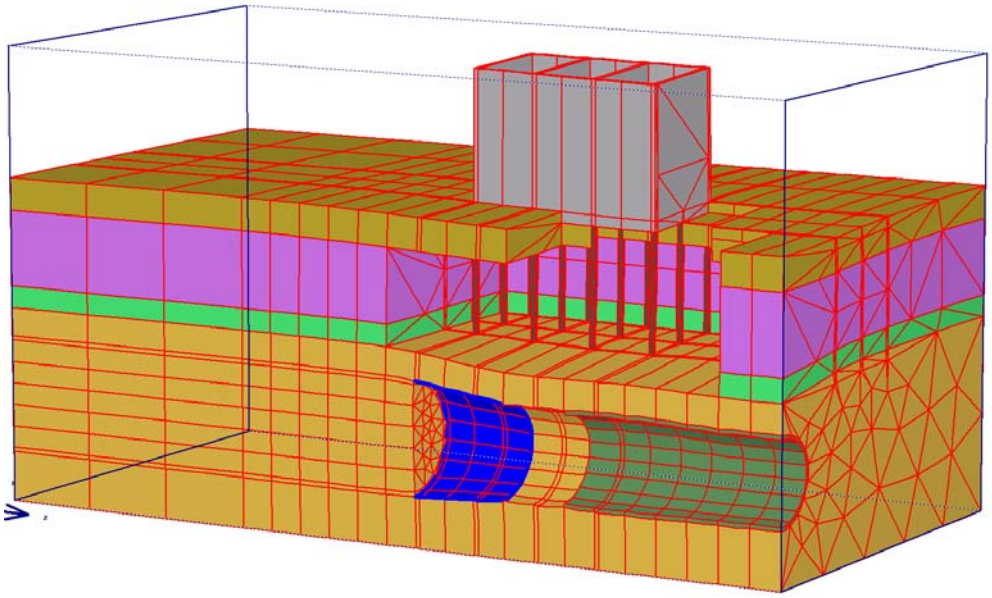

Figure 6. Partial view of the deformed mesh at the end of Phase 15
(deformations enlarged 50 times)

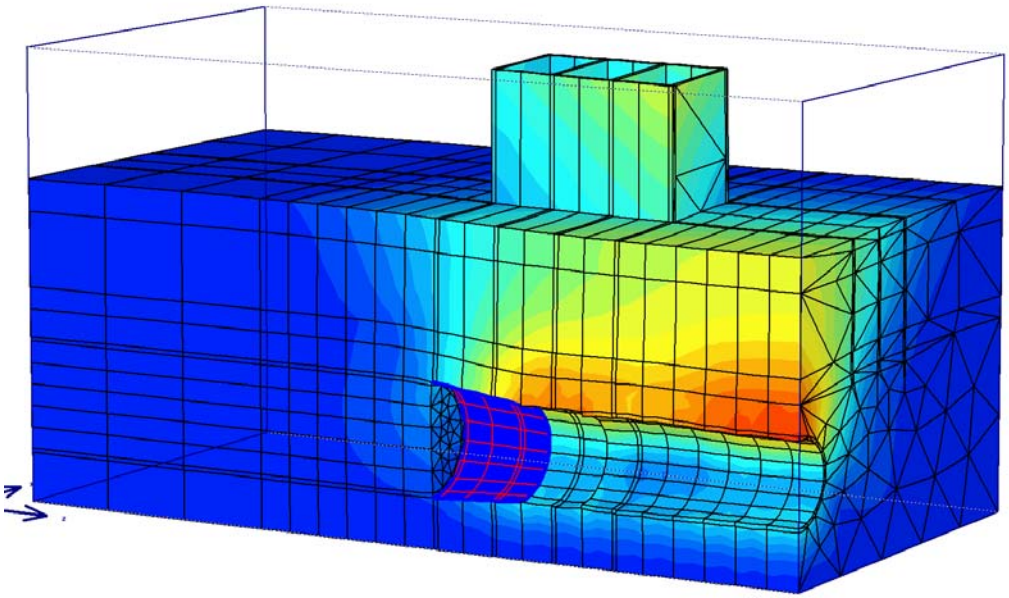

Figure 7. Shadings of total displacements at the end of Phase 15
(deformations enlarged 50 times)

The far back corner of the building on the other hand has displaced only 10 mm at this point. The torsion the building is subjected to, can be seen from a plot of the shear strains in the building, see Figure 8.

Once the TBM has passed the last row of piles, the remaining houses also settle into the settlement trough. The shearing of the buildings in the longitudinal direction is reduced then. At the end, as the first lining ring is installed next to the piles, the maximum shear strain remaining is about 1%.

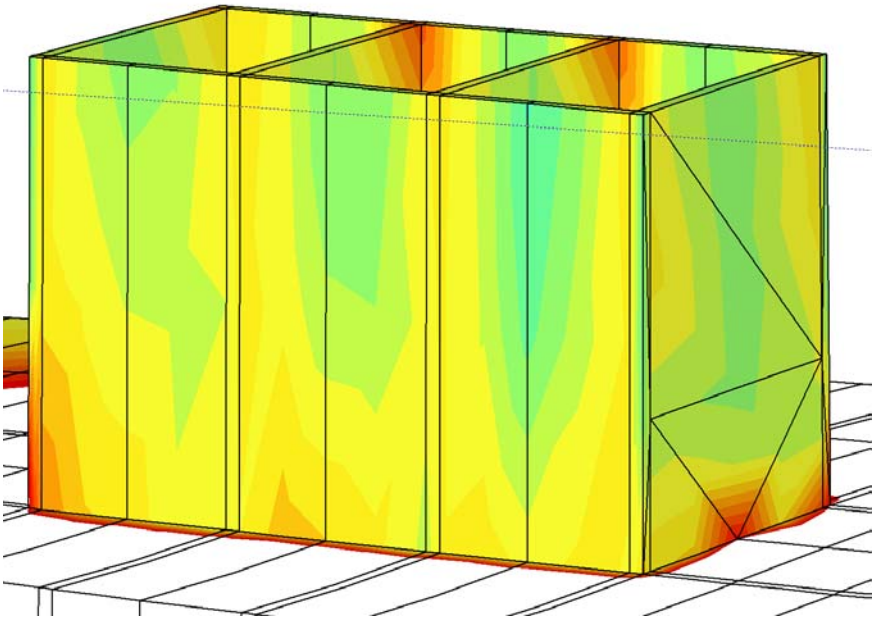

Figure 8. Shaded plot of shear strains in the building as the TBM passes the last row of piles (deformations enlarged 50 times)

4. Conclusions

The deformations occurring during tunnel construction around a tunnel boring machine can be predicted with good accuracy using a phased excavation scheme in a 3D finite element calculation. This phased excavation scheme includes the effects of the support pressure at the tunnel face, the conicity of the shield as well as the grouting pressure at the shield tail. The tunnel boring process is simulated by advancing the tunnel boring machine stepwise through the model. The settlement trough calculated in this way is less wide and steeper than found from 2D finite element calculations.

For the case of the Second Heinenoord tunnel the deformations calculated with this scheme have been compared with field observations. The width and shape of the surface settlement trough is predicted with good accuracy. Also the deformations in the subsoil correspond well with observations from inclino- and extensometers, where it is observed that the deformations at depth are larger than at the surface.

The same excavation scheme has been used to study the influence of tunnel boring on a number of masonry building founded on piles. A row of 4 houses has been modelled using volumetric elements. As the tunnel boring machine passes the houses the corner closest to the tunnel boring machine settles more and earlier than the remainder of the houses. The resulting torsion of the houses can be observed from the strains in the buildings.

5. References

Bakker K.J., van Scheldt W. Plekkenpol J.W. (1996) Predictions and a monitoring scheme with respect to the boring of the Second Heinenoord Tunnel. Geotechnical aspects of underground construction in soft ground. Balkema, Rotterdam, 459-464.

Brinkgreve R.B.J., Vermeer P.A. (2001) Plaxis 3D Tunnel (Validation manual). Balkema, Lisse.

COB Centre for Underground Construction (1996) Parameterset voor de predicties, COB Report K100-W-004. Gouda

Strack O.E., Verruijt A. (2000) A Complex Variable Solutions for the Ovalization of a Circular Tunnel in an Elastic Half-Plane. GeoEng2000, An International Conference on Geotechnical & Geological Engineering. Technomic.

Teunissen E.A.H., Hutteman M. (1998) Pile surface settlements at full scale tests North/South metro line. Tunnels and Metropolises, WTC '98. Balkema, Rotterdam

Vermeer P.A., Ruse N. (2000) Face stability when tunneling in soil and homogeneous rock. Proc. Developments in Theoretical Soil Mechanics – The John Booker Memorial Symposium. Sydney, 123-138.

Vermeer P.A. (2001) On a smart use of 3D-FEM in tunnelling. Plaxis Bulletin (11), 2-7

Verruijt A., Booker J.R. (200) Complex Variable Analysis of Mindlin's Tunnel Problem. Proc. Developments in Theoretical Soil Mechanics – The John Booker Memorial Symposium. Sydney, 3-22.

Van der Vliet C., de Boer A., Blom C.B.M., Ros P.L.M. (2001) Strategy and results of calibration for complex 3D finite element model for tunnel linings in soft soil. Modern Tunneling Science and Technology. Swets & Zeitlinger, 835-838.